DISRUPTION OF METAL MELT CONNECTIVITY IN A PARTIALLY MOLTEN SILICATE MATRIX.

K. B. Prissel[1] and Y. Fei[1], [1]Earth and Planets Laboratory, Carnegie Institution for Science, 5241 Broad Branch Road NW, Washington, D.C. 20015, kprissel@carnegiescience.edu

Introduction: Metal-silicate differentiation on small planetary bodies involves the separation of metal melt from a silicate matrix. The efficiency and timing of metal segregation control the metal distribution in a planetary body. For small planetary bodies that do not experience enough heating to melt the silicate portion, metal melt percolation in a solid silicate matrix is the primary mechanism of metal segregation.

Generally, metal melt percolation is considered energetically feasible when the dihedral angle of the metal melt, which is a function of its interfacial energy, is below a critical value of 60°. Previous studies indicate that an increased volume proportion of metal and increased abundance of light elements (i.e., O, S, C) in the metal decrease the metal melt dihedral angles (e.g., [1-3]). In-situ conductivity measurements of metal- and silicate-bearing experiments have demonstrated that the presence of silicate melt disrupts the connectivity of Fe-S metal melt in a peridotite matrix [4].

Though planetesimals with a radius >20 km likely melted to some extent during accretion [5], the extent of melting is dependent not only on the terminal radius of the planetary body, but also the timing and duration of accretion. For instance, a planetary body with 1500 km radius that accreted 5 Myr after the formation of CAIs will not have enough radioactive heating to fully melt the silicate portion [6]. For cases in which the silicate portion of a planetary body is partially molten during differentiation, it is important to identify the effect of silicate melt on the mechanics of metal segregation. In this study, we conduct experiments over a range of temperatures and metal melt proportions in order to investigate the effect of partial melting on the connectivity of Fe-S metal melt in a silicate matrix.

Methods: Piston cylinder experiments were conducted using two silicate matrices: natural San Carlos olivine powder (SCO) and synthetic Kilbourne Hole peridotite (KLB-1). For SCO, natural olivines were hand-separated from a San Carlos xenolith sample and then ground to a powder. The KLB-1 peridotite sample was synthesized by sintering a pre-conditioned mixture of oxides in a Au capsule and ¾" talc-Pyrex assembly at 1 GPa and 1000°C for 24 hours. The metal mixture was prepared from Fe and FeS powders to match the Fe-S eutectic composition at 1 GPa. Two metal proportions were investigated (10 vol.% and 18 vol.%) and metal-silicate mixtures were ground under ethanol for 30 minutes. The samples with 18 vol.% metal were doped with 2 wt.% W metal powder.

Metal percolation experiments were conducted using a ½" talc-Pyrex assembly in the piston-cylinder apparatus and consisted of two MgO capsules: one with a SCO matrix, one with a KLB-1 matrix. Metal-silicate mixtures were loaded into MgO capsules, and then topped with Pt foil and an MgO lid. For each experiment, the two MgO capsules were stacked within a sealed Pt capsule. The experiments were conducted at 1 GPa and temperatures ranging from 1100°C to 1300°C. Run durations varied from 6 hours to 24 hours in order to assess the extent of chemical and textural equilibration. Experimental run products were analyzed with a JEOL JXA-8530F electron microprobe at Carnegie Earth and Planets Laboratory and the data were processed using Probe for EPMA software.

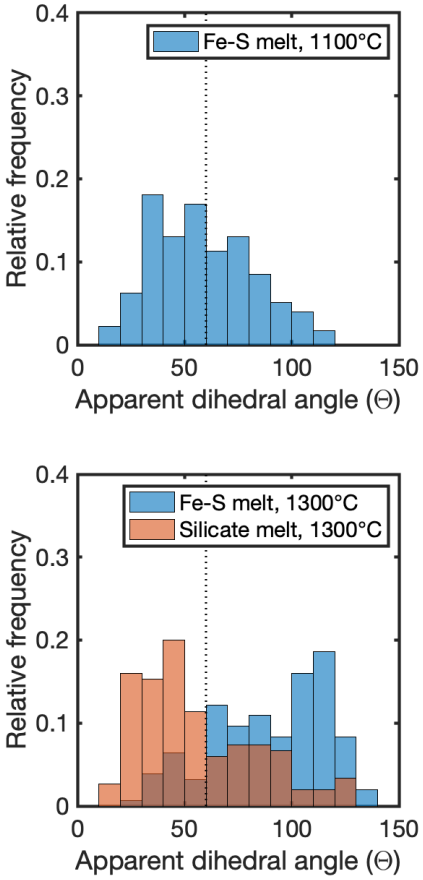

Figure 1. Apparent dihedral angle measurements for Fe-S and silicate melts in a peridotite matrix at 1100°C (top) and 1300°C (bottom). The dashed line marks the percolation threshold of 60°. The presence of silicate melt at 1300°C leads to a median dihedral angle >60° for the Fe-S melt.

Metal melt connectivity: Two methods were used to assess the extent of metal melt connectivity: Pt element mapping and dihedral angle measurements. Our group recently developed the use of Pt EDS mapping as a proxy for melt connectivity [7]. Capping the MgO capsule with Pt foil provides a source of Pt for each sample. During the experiment, the Pt foil reacts with Fe metal in the sample. If the Fe metal forms an interconnected network in the silicate matrix, then Pt diffuses throughout the sample via the metal melt network. Thus, mapping the Pt distribution in the sample gives insight into whether or not the metal was interconnected during the experiment. In addition to Pt EDS mapping, apparent dihedral angles were measured from backscattered electron images of the quenched experimental samples using the angle tool in ImageJ.

For 18 vol.% metal in a KLB-1 matrix, our experiments indicate that the metal melt was interconnected at 1100°C and not interconnected at 1300°C (Figure 1). Below the KLB-1 solidus (1100°C), the median of the apparent dihedral angle measurements for Fe-S melt is less than 60°, which is favorable for building a connected metal network in the peridotite matrix. EDS mapping of the experimental charge shows Pt distributed throughout the sample, providing further evidence for an interconnected metal network during the experiment. Above the solidus (1300°C), the median of the measured dihedral angles for Fe-S melt is greater than 60°, indicating that the presence of silicate melt disrupted the interconnected network of metal melt. Additionally, Pt is concentrated at the top of the capsule near the Pt foil and does not appear to have diffused throughout the sample. For the silicate melt, the median of the measured dihedral angles is less than 60°.

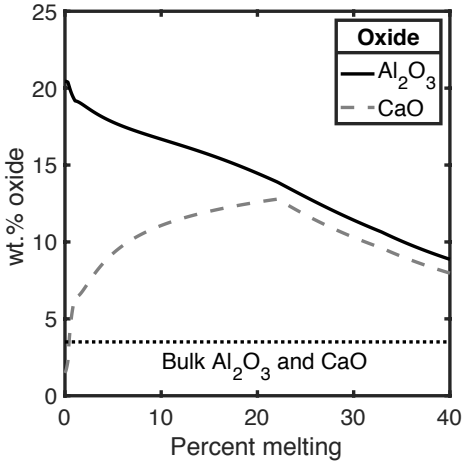

Figure 2. Silicate melt composition during partial melting of KLB-1 bulk composition modeled at 1 GPa and fO_2 = IW using alphaMELTS [11].

For samples with 10 vol.% metal, the metal melt was not interconnected in either the 6 hour or 24 hour experiment. For a similar Fe-S melt composition and KLB-1 silicate matrix at 1 GPa, [4] found that >5 vol.% metal was needed in order to form a metal melt network, whereas a connected network existed only for metal proportions >15 vol.% in [3]. Our results are consistent with those of [3], with metal proportions >15 vol.% required for an interconnected metal melt network.

Implications for core formation on small planetary bodies: Our results indicate that partial melting of a silicate matrix disrupts the metal melt network. This disruption has been noted to occur even at 26 vol.% metal [4]. Though silicate melting prohibits metal segregation by percolative flow of metal melt, melting promotes metal segregation by forming silicate melt channels through which metal droplets may be transported [8]. Moving forward, it is important to identify the percolation threshold as a function of degree of partial melting. This will have implications for the dynamics of core formation on small planetary bodies, as well as for metal-bearing systems that have experienced silicate melting, such as those preserved in the ureilites [9] and lodranites [10].

Effect of silicate melting on metal-silicate partitioning. If metal melt is transported as droplets in silicate melt channels, then the relevant metal-silicate partitioning is that between the metal melt and silicate partial melt. The composition of the silicate melt will differ from the bulk silicate composition of the planetary body, especially at low degrees of partial melting (Figure 2). For example, in our 1300°C experiment, the bulk Al_2O_3 and CaO contents were each approximately 4 wt.%, whereas the silicate melts coexisting with Fe-S melt contain up to 15 wt.% Al_2O_3 and 10 wt.% CaO. Metal segregation in a partially molten silicate matrix may influence the bulk mantle distribution of elements whose metal-silicate partitioning is strongly affected by silicate melt composition, such as W, Mo, and P (e.g., [12-14]).

References: [1] Holzheid et al. (2000) *JGR, 105,* 13555–13567. [2] Terasaki et al. (2008) *EPSL, 273,* 132-137. [3] Bagdassarov et al. (2009) *PEPI, 177,* 139-146. [4] Yoshino et al. (2004) *EPSL, 222,* 625-643. [5] Elkins-Tanton (2012) *Annu. Rev. Earth Planet. Sci., 40,* 113–139. [6] Šrámek et al. (2012) *Icarus, 217,* 339-354. [7] Wang and Fei (2020) *AGU Fall Meeting,* DI019-0006. [8] Stevenson (1990) *Origin of the Earth*, 231-250. [9] Mittlefehldt et al. (1998) *RiMG, 36,* 4.1-4.195. [10] Taylor (1992) *JGR, 97,* 14717-14726. [11] Smith and Asimow (2005) *G3*, *6,* Q02004. [12] Walter and Thibault (1995) *Science, 270,* 1186-1189. [13] Jana and Walker (1997) *EPSL, 150,* 463-472. [14] O'Neill et al. (2008) *Chemical Geology, 255,* 346-359.